TRITA-MEK - - 93 - 16
Technical Report 1993:16
ISSN 0348-467X
ISRN KTH/MEK/TR--93/16-SE

# Experiments in a boundary layer subjected to free stream turbulence
## Part I: Boundary layer structure and receptivity

K.J.A. Westin, A.V. Boiko, B.G.B. Klingmann,
V.V. Kozlov & P.H. Alfredsson

TRITA-MEK --93-16
Technical Report 1993:16
ISSN 0348-467X
ISRN KTH/MEK/TR--93/16-SE

# Experiments in a boundary layer subjected to free stream turbulence
## Part I: Boundary layer structure and receptivity

K.J.A. Westin, A.V. Boiko, B.G.B. Klingmann,
V.V. Kozlov & P.H. Alfredsson

December 1993
Technical Reports from the
Royal Institute of Technology
Department of Mechanics
S-100 44 Stockholm, Sweden

# Experiments in a boundary layer subjected to free stream turbulence.
# Part I: Boundary layer structure and receptivity.

K.J.A. WESTIN[1], A.V. BOIKO[2], B.G.B. KLINGMANN[1],
V.V. KOZLOV[2] & P.H. ALFREDSSON[1]

[1]Dept. Mechanics/Fluid Physics, Royal Institute of Technology, S-10044 Stockholm, Sweden
[2]Dept. Theoretical and Applied Mechanics, Russian Academy of Sciences, Siberian Branch, 630090 Novosibirsk, Russia.

**Abstract**

The modification of the mean and fluctuating characteristics of a flat plate boundary layer subjected to nearly isotropic free stream turbulence (FST) is studied experimentally using hot-wire anemometry. The study is focussed on the region upstream of the transition onset, where the fluctuations inside the boundary layer are dominated by elongated flow structures which grow downstream both in amplitude and length. Their downstream development and scaling is investigated, and the results are compared to those obtained by previous authors. This allows some conclusions about the parameters which are relevant for the modelling of the transition process. The mechanisms underlying the transition process and the relative importance of the Tollmien-Schlichting wave instability in this flow are treated in an accompanying paper (part II of the present report).

## 1 Introduction

Despite being a subject of interest since the thirties, the effect of free stream turbulence (FST) on the onset of transition has received detailed attention only since the last few years. This problem is of great interest in applied engineering, for instance for the prediction of transition on turbine blades, where the impingement of turbulence from the wake of the stator influences the boundary layers on the rotor blades. Another important aspect is the influence of FST on wind-tunnel experiments in general (both sub- and supersonic). It is desirable to reduce the FST-level in order to resemble free-flight conditions, but all wind-tunnels have some background disturbances with different characteristics, and more knowledge about the 'dangerous' FST-parameters will be of interest. Attempts have been made by several authors to establish empirical correlations between the free stream turbulence and the transition Reynolds number. At FST levels ($Tu$) above 5%, transition occurs at the minimum Reynolds number where self-sustained boundary layer turbulence can exist, i.e. at $Re_\theta \approx 190$ where $Re_\theta$ denotes the Reynolds number based on momentum loss thickness (see Arnal, 1992, for a review). At lower levels of FST, however, different experiments disagree widely as to the location and extent of the transition region, and there seems to be no general correlation between the level of the free stream turbulence and the location of transition onset. Neither can the transition Reynolds number be found by merely taking into account the

fluctuations inside the boundary layer. Transition is also sensitive to a large number of other parameters, including not only the overall level of FST but also spatial scales, degree of isotropy and homogeneity, conditions at the leading edge of the model, presence of pressure gradients, etc., each of which requires special attention. Depending on these conditions, FST-induced transition may be caused by different types of boundary layer instabilities. These can be Tollmien-Schlichting (TS) waves and other, not yet completely understood phenomena, which require different modelling approaches. The basic problem in modelling FST induced transition, as pointed out by Arnal, is the lack of understanding of the transition mechanisms at work.

For engineering purposes, recent attempts have been made to model the transition in the presence of FST by transport equations. Most transport models rely on a transition criterion, usually derived from an empirical correlation, for modifying the closure parameters through the transition region. If transition is to be modelled without resorting to empirical correlations, it is necessary to correctly reproduce the laminar flow characteristics upstream of the onset of transition. An extensive comparison of numerical methods, using the experiments by Roach & Brierley (1992) as a reference (the so-called T3 test cases), was made during the 'Workshop on Transition and Turbulence in Lausanne' (see Pironneau et al., 1992). From the results presented at this Workshop, it is clear that transport models are unable to reproduce the structure of the laminar boundary layer fluctuations needed for the closure of the equations.

So far, only a few experimental studies have reported measurements of the mean velocity in the region upstream of transition for boundary layers subjected to FST. Nor have comparisons been made between fluctuation characteristics obtained in different experiments, despite the fact that such experimental data usually are presented. Because of the lack of knowledge about the effect of different parameters involved, it is necessary to be careful when drawing conclusions from results obtained under different experimental conditions. In the present experiments, special care was taken to create 'standard' experimental conditions: a zero pressure gradient, control of leading edge conditions, a low level of uncontrolled free stream disturbances (both sound and turbulence), and isotropy of the grid generated turbulence.

This paper is organized as follows: A brief overview of previously known results on the receptivity of the boundary layer to FST is given below. The experimental set-up is described in section 2, and the free stream characteristics are discussed in section 3. Results of investigations of the boundary layer structure are presented in section 4, and discussed in section 5 together with previous author's findings. The main conclusions from this study are summarized in section 6.

## 1.1 Brief overview of the boundary layer receptivity to FST

The first detailed measurements concerning the development of a laminar boundary layer in the presence of FST were presented by Arnal & Juillen (1978). They observed a downstream growth of the streamwise velocity fluctuations ($u_{rms}$), reaching amplitudes of several percent of the free stream velocity ($U_0$) before the onset of transition. They also found that the energy spectrum inside the boundary layer is dominated by contributions at much lower frequencies than in the turbulent free stream. The distribution of $u_{rms}$ across the boundary layer was quite different from that of TS-waves (e.g. the maximum was found near the middle of the boundary layer instead of near the wall as for TS-waves). Waves with frequencies typical of unstable TS-waves were also seen riding on the large scale (low-frequency) structures, however, their amplitudes were small compared to the overall fluctuation level. Later studies by Kendall (1985, 1990, 1991) were focussed on the receptivity and development of wave packets induced by FST at $Tu$ between 0.1% and 0.2%. At higher disturbance levels the TS-waves become difficult to detect, and their role in transition is

therefore not evident. Recent experiments by Blair (1992), carried out in accelerating flows at a high ambient disturbance level, show that transition can also occur under conditions which are subcritical with respect to TS-waves.

The boundary layer perturbations were investigated at larger FST levels in experiments by Kosorygin et al. (1982) and Kosorygin & Polyakov (1990), who found that the shape of the $u_{rms}$-profile is nearly independent of both $Tu$ and the Reynolds number. The spanwise and wall-normal scales of the low frequency structures were of the order of the boundary layer thickness, and the amplitude of normal velocity fluctuations ($v_{rms}$) inside the boundary layer was several times smaller than $u_{rms}$. Flow visualizations (Kendall, 1985; Gulyaev et al., 1989) show that the low frequency fluctuations in the boundary layer are caused by longitudinal streak structures which start to develop from the leading edge of the plate. It should be emphasized that the observed boundary layer perturbations with a dominating streaky pattern, although random in time and space, are not what we usually call turbulence.

Suder, O'Brien & Reshotko (1988) and Roach & Brierley (1992) directed their attention to the transition region itself. In the experiments by Suder et al., transition was observed at remarkably low Reynolds numbers compared with other experiments made under similar conditions, and turbulent spots appeared at relatively low fluactuation levels in the boundary layer (3-4% of $U_0$). The onset of turbulence is accompanied by a rather well defined increase in the wall shear stress, and can also be clearly seen in the fluctuating velocity profiles, which develop a distinct near wall maximum due to the turbulent motion. Irrespective of the dominant mechanism responsible for the transition, which may have been different in all the above mentioned cases, the transition region is characterized by a random appearance of turbulent spots which grow in number and size downstream, until the boundary layer becomes fully turbulent.

So far, neither the receptivity nor the growth mechanism of the observed longitudinal structures have been identified, and their precise role in the transition to turbulence is not clear. The receptivity of the boundary layer to free stream disturbances can be investigated by generating controlled 'model' disturbances in the free stream, and studying the subsequent development of perturbations inside the boundary layer. Such experiments by Grek et al. (1985, 1991) have shown that a transient localized disturbance upstream of the leading edge can initiate the development of unstable flow structures in the boundary layer in the same way as transient disturbances introduced from the wall or in the interior of the boundary layer. After an initial development, these structures develop into turbulent spots, provided that the initial disturbance is large enough. These 'incipient spots' have been extensively studied both theoretically, experimentally and numerically (cf. Gustavsson, 1991; Grek et al.; Klingmann, 1992; Henningson, Lundbladh & Johansson, 1993). They are characterized by an algebraic energy growth and weak spanwise spreading. The spanwise streak spacing of an incipient spot depends on the initial disturbance causing it, but is typically of a size comparable to the boundary layer thickness.

A critical part of the experimental set-up is the leading edge of the plate. A slightly non-uniform pressure distribution at the leading edge can have a substantial effect on TS-wave amplification (see Klingmann et al., 1993). The effect of different leading edge bluntness in the presence of FST was investigated by Kendall (1991). It was found that the amplitude of waves in the TS-wave frequency band was much higher in the case of a blunt leading edge, while the amplitude of the low frequency perturbations was not affected. The generation of turbulent spots at the leading edge is also affected by the shape and the pressure distribution at the leading edge, where small (unstationary) separation bubbles will favour the formation of turbulent spots. This was studied in an experiment by V.E. Kozlov et al. (1990), where local separation was attenuated by a small negative angle of attack, resulting in a downstream movement of the transitional Reynolds number. By rounding

the leading edge, the same effect could be obtained at a smaller negative angle of attack.

An observation made at the Lausanne Workshop is the sensitivity to the specified free stream characteristics. The structure of grid-generated FST depends on the free stream velocity and flow quality upstream of the grid, the grid geometry, as well as on how the grid is installed. In most transition experiments, the turbulence level is described in terms of the rms-level and the spectral distribution of the streamwise velocity component ($u$) in the free stream. In a numerical study by Yang & Voke (1990), different free stream conditions were imposed, and it was found that free stream fluctuations in the pressure ($p$) and normal velocity ($v$) are the most efficient in exciting perturbations in the boundary layer, whereas fluctuations in the streamwise velocity ($u$) are rather harmless. Unless the FST is isotropic, the scales and intensity of the $v$-component can not be obtained from the frequency spectrum of $u$. If the grid is installed in the settling chamber, as in the experiments of Kendall (1985, 1990, 1991) and Suder et al. (1988), the streamwise fluctuations are suppressed more efficiently than the transverse fluctuations when the flow passes through the contraction. This gives an anisotropy in the FST, which decays along the test section. In such a case, it is necessary to study the cross stream scales, in order to asses the precise characteristics of the FST.

## 2 Experimental set-up and measurement technique

The experiments were performed in the MTL (Minimum Turbulence Level) wind tunnel at the Royal Institute of Technology (KTH), Stockholm, Sweden. It is a closed return tunnel, with a 7 m long test section of 0.8 x 1.2 m cross section, preceded by a contraction with ratio 9:1. One of the particular features of this tunnel is the low level of free stream turbulence in the test section, where the intensity of the streamwise velocity fluctuations is below 0.02% in the velocity interval 10-60 m/s (see Johansson, 1992). The experimental setup as well as the measurement parameters are matched to the experiments by Klingmann et al. (1993) for an undisturbed flat plate boundary layer flow at zero pressure gradient - in fact some of the measurements were carried out simultaneously.

A general sketch of the setup is shown in figure 1. The experiments were carried out on a 2.16 m long flat plate (called set-up I) or a 4.22 m long plate (set-up II). Set-up I is identical to that described in Klingmann et al. (1993). The streamwise, wall-normal and spanwise directions are denoted $x$, $y$ and $z$ respectively. Measurements were undertaken in the region between 100 and 1000 mm from the leading edge ($x = 0$), at free stream speeds ($U_0$) between 4 m/s and 8 m/s. The Reynolds number, defined as $R = 1.72\sqrt{U_0 x/\nu}$ where $\nu$ is the kinematic viscosity, was between 200 and 1260. The test section walls were adjusted to obtain a zero streamwise pressure gradient along the plate. The pressure variations, obtained by measuring $U_0$ near the edge of the boundary layer, and then evaluating the pressure from Bernoulli's equation, were constant to within 1% of the dynamic pressure along the plate.

FST was generated by a grid, installed in the test section 1.5 m upstream of the leading edge of the plate. The mesh size and the wire diameter of the grid were 23.5 mm and 3.5 mm respectively, giving a solidity of 0.28 (the solidity is defined as the grid blockage area over the total area). This resulted in a fairly isotropic turbulence with a level of $Tu$ about 1.5%. A detailed description of the grid generated turbulence is given in section 3. With the grid installed, turbulent spots were occasionally observed at $x = 1000$ mm and $U_0 = 8$ m/s. This position can be said to correspond to the beginning of the transition region.

The leading edge of the flat plate is one of the critical points in the design of the experiment, since the receptivity may be influenced even by non-uniformities which are small enough to have a negligible effect on the boundary layer development. A uniform pressure distribution near the

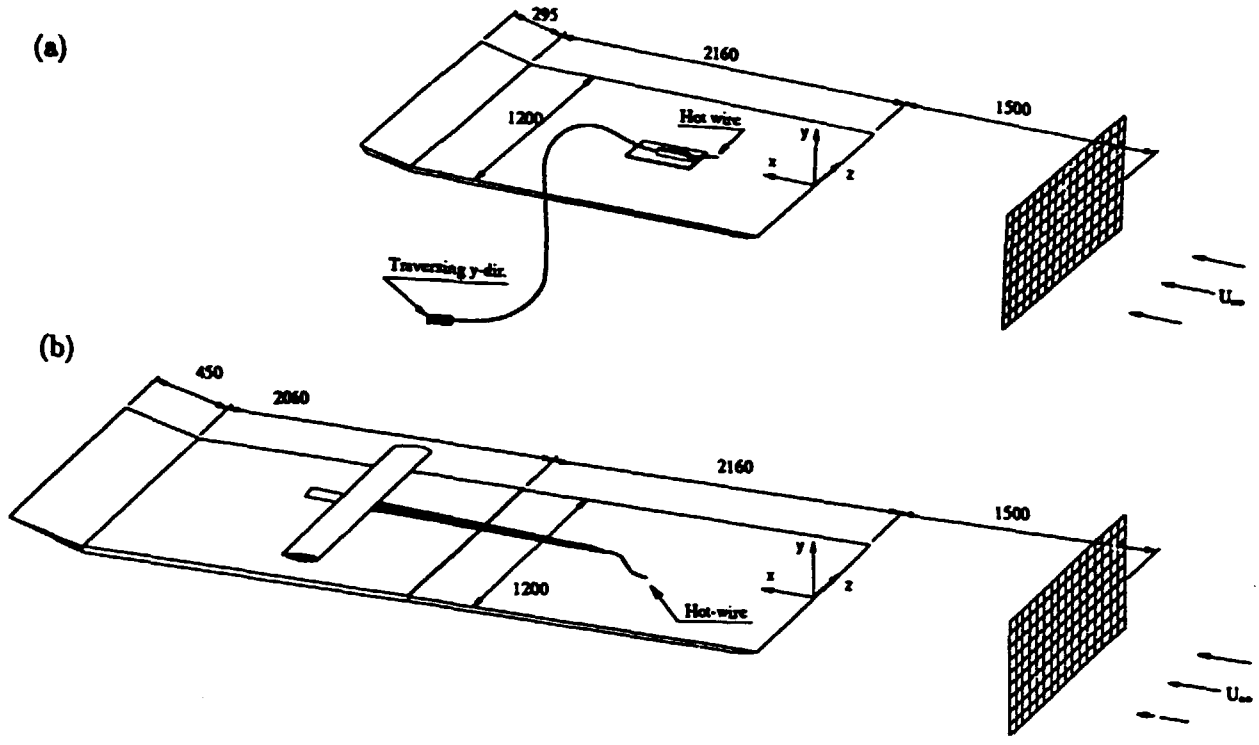


Figure 1: Outline of experimental set-up (a) set-up I, (b) set-up II.

leading edge can usually not be obtained using elliptic or wedge-shaped leading edges, although careful attention to this problem can minimize undesirable effects. The presence of the grid may enhance the tendency for the formation of a suction peak near the leading edge, and also induces an unsteadiness of the pressure distribution. In the present setup, a smooth pressure distribution was achieved by a special design of the leading edge (see figure 2a) in combination with a trailing edge flap for adjustment of the stagnation line (see also Klingmann et al., 1993). The importance of leading edge effects can be appreciated from a simple observation made during the preparations of the experiment: When the trailing edge flap was lowered, the stagnation point moved to the reverse side of the plate, resulting in a strong suction peak on the working side. The peak level was about 10% of the dynamic pressure, and affected the region $x < 200$ mm. With the grid installed, the flow was then fully turbulent already at $x = 500$ mm and $U_0 = 8$ m/s. After adjustment of the flap, the transition point was moved downstream of the last measurement position ($x = 1000$ mm).

Figure 2b shows the pressure distribution near the leading edge in the absence of the grid, after adjustment of the flap. The pressure coefficient, defined as

$$C_p = \frac{p - p_{ref}}{p_0 - p_{ref}}$$

where $p$ is the local static pressure, $p_{ref}$ the static pressure at a reference point on the plate and $p_0$ the total pressure, was evaluated from measurements with a static pressure tube positioned in the vicinity of the boundary layer. The pressure smoothly decreases within the first 20 mm, as the flow accelerates from the stagnation point. The pressure distribution was only slightly affected by the

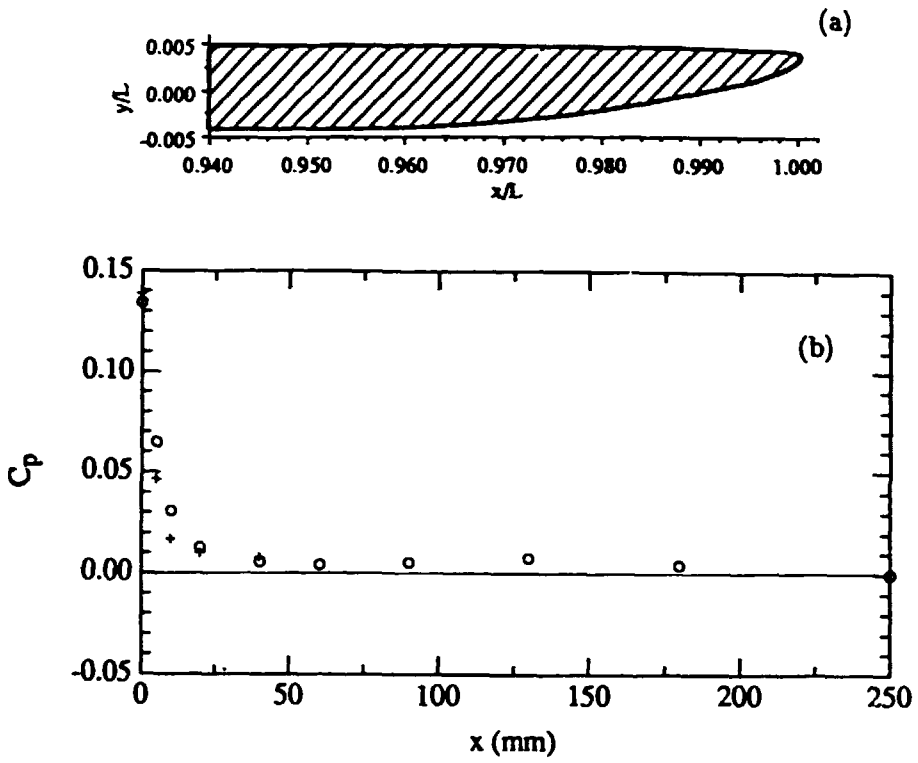


Figure 2: (a) Leading edge of the flat plate. Reference length L=2 m. (b) Distribution of the pressure coefficient ($C_p$) along the plate. Reference position $x = 250$ mm. Static pressure tube traversed at (o) $y = 5$ mm, (+) $y = 2$ mm.

presence of the grid. After inserting the grid, a small decrease in the pressure ($\Delta C_p < 1.5\%$) was observed within the first 25 mm from the stagnation point. Compared to set-ups reported in other studies, the departure from a perfect zero pressure gradient near the leading edge is quite small, and it is also confined to a smaller region. For instance, in the set-up of Arnal & Juillen (1978) the leading edge of their body of revolution gave a suction peak of 10%, and Roach & Brierley (1992) report pressure deviations amounting to about 3% on the wedge-shaped leading edge used in their experiment.

The streamwise and normal velocities were measured with constant-temperature hot-wire anemometers, using both single and cross wire probes. The single wires were made of 5 $\mu$m platinum wire with a sensing length of 1 mm, operating at 60% overheat, and calibrated with a Prandtl tube in the free stream. A calibration function of the form

$$U = k_1(E^2 - E_0^2)^{1/n} + k_2(E - E_0)^{1/2}$$

was used, where $E$ and $E_0$ are the anemometer output voltages at the velocities $U$ and zero respectively, and $k_1$, $k_2$ and $n$ are constants to be determined for the best fit to the calibration data. The value of $n$ is usually close to 0.5. The second term represents the contribution from free convection at low velocities, and makes it possible to extrapolate the calibration curve to low velocities. A cross-wire probe, used for measurements of both the streamwise and transverse velocity components in the free stream, was made of 2.5 $\mu$m wires and had a measurement volume smaller than 0.5 mm in side length. The probe was calibrated at different angles and flow velocities, from which $u$ and $v$ were calculated, and a voltage pair $(E_1, E_2)$ was obtained at each calibration

point. Two third degree polynomial surfaces were then fitted to the calibration data, giving $u$ and $v$ as functions of $(E_1, E_2)$.

Temperature variations within 1° were accounted for by compensating the output voltage from the anemometer by a factor

$$E_{corr} = \frac{E}{\sqrt{1 - \frac{\Delta T}{T_s - T_f}}}$$

where $E$ and $E_{corr}$ denote the measured and corrected voltages respectively, $T_s$ is the sensor temperature, $T_f$ is the fluid temperature and $\Delta T$ is the temperature drift.

The probes were traversed in the following two different ways. In set-up I the probe was supported by an 82 mm long rod and was traversed in the $y$-direction (normal to the wall) by means of a wedge mechanism moveable with a micrometer screw and operated via a speedometer wire from outside the tunnel. The accuracy of the hot-wire position with this mechanism was about 0.02 mm. In some later measurements (setup II) a newly constructed traversing mechanism made it possible to traverse the probe in all three directions with an accuracy of 0.01 mm. This system was used for all X-wire measurements. In order to avoid interference between the trailing edge flap and the traversing mechanism, the initial plate was prolonged with an extension plate to a total length of 4.22 m.

# 3 Characteristics of the free stream turbulence

In order to investigate the boundary layer receptivity, it is necessary to have a good characterization of the FST. Its structure depends on several parameters, for instance the free stream velocity and flow quality upstream of the grid, on the geometry of the grid and on how it is installed. The low level of background turbulence and sound in the MTL wind tunnel allows a good control of the free stream conditions. The grid was placed in the test section, 60 mesh widths upstream of the flat plate leading edge. Grid generated turbulence is usually assumed to become isotropic after 20 mesh widths, however, some studies indicate that a small anisotropy may survive over 400 mesh widths downstream (see Groth & Johansson, 1988, for a more extensive discussion), and this was also found to be the case in the present set-up. This affects the ratios between $u$ and $v$, and between the transverse and longitudinal turbulent scales. The interest is here focussed on the Taylor micro scale and the integral scale, which may be assumed to be the most relevant for the boundary layer receptivity.

The turbulence level $Tu$ is here defined as $u_{rms,0}/U_0$, where $u_{rms,0}$ is the rms-level of $u$ in the free stream, measured close to the leading edge ($x = 0$). $Tu$ was 1.5% at $U_0 = 8$ m/s and 1.35% at $U_0 = 4$ m/s, and its variation with $U_0$ was approximately linear within this velocity range. Figure 3a shows the spectral density of $u$ for $U_0 = 4$ and 8 m/s, plotted versus the non-dimensional frequency F, defined as $2\pi f\nu \cdot 10^6/U_0^2$. The spectral density ($E$) is here defined as the spectral power normalized by $0.5U_0^2\Delta F$ ($\Delta F$ is the frequency resolution), and is therefore independent of the sampling parameters. From figure 3a it is clear that the relative energy distribution is shifted slightly towards higher F when the velocity is decreased. The turbulent scales can be compared by looking at the autocorrelations of $u$ ($R_{uu}$) for the two velocities (figure 3b). Using Taylor's hypothesis, the time separation ($\Delta t$) was translated into a longitudinal space separation ($\Delta x$) by multiplication with $U_0$. The correlation functions are quite similar for both velocities, indicating that there are only minor differences in the turbulent scales.

Figure 4a compares the spectral density of the $u$ and $v$ fluctuations in the free stream, measured

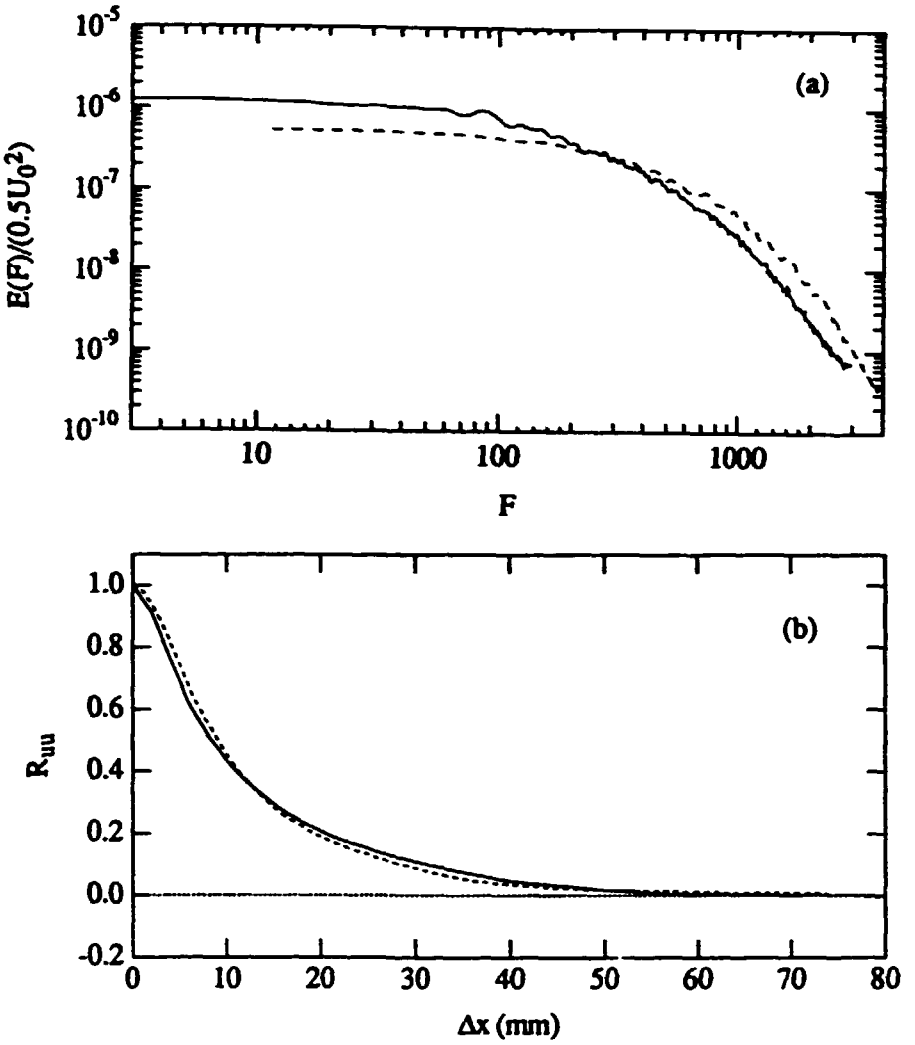


Figure 3: (a) Free stream spectra and (b) autocorrelation of $u$ at $x = 0$. (---) $U_0 = 4$ m/s, (—) $U_0 = 8$ m/s.

with an X-wire probe at $x = 0$ and $U_0 = 8$ m/s. In agreement with the theory for isotropic turbulence, the energy of $u$ is shifted to lower frequencies than the $v$-spectrum. In order to assess the degree of isotropy and the typical transverse scales in the free stream, the FST was investigated in more detail at $U_0 = 8$ m/s. A relevant test of the isotropy of the scales is to compare the spatial correlations in different directions. Two-probe cross-correlations of $u$ were measured in the free stream at $x = 500$ mm, using separations in both $y$ and $z$. This gives the transversal correlation in the crossflow directions. These results are shown in figure 4b together with the autocorrelation of $v$, obtained from the frequency spectrum. By using Taylor's hypothesis, the autocorrelation curve can be interpreted as a transversal correlation in the streamwise direction. The good agreement between the three correlation curves shows that the fluctuation scales are near isotropic. The autocorrelation of $u$, which is the same as shown in figure 3b, is also shown for reference.

The turbulent micro scale $\tau$ (Taylor time scale) gives an estimate of the smallest energetic eddies in the turbulence. It can be estimated directly from the autocorrelation, but here it was calculated as the ratio between the turbulent rms-fluctuations and their time derivatives,

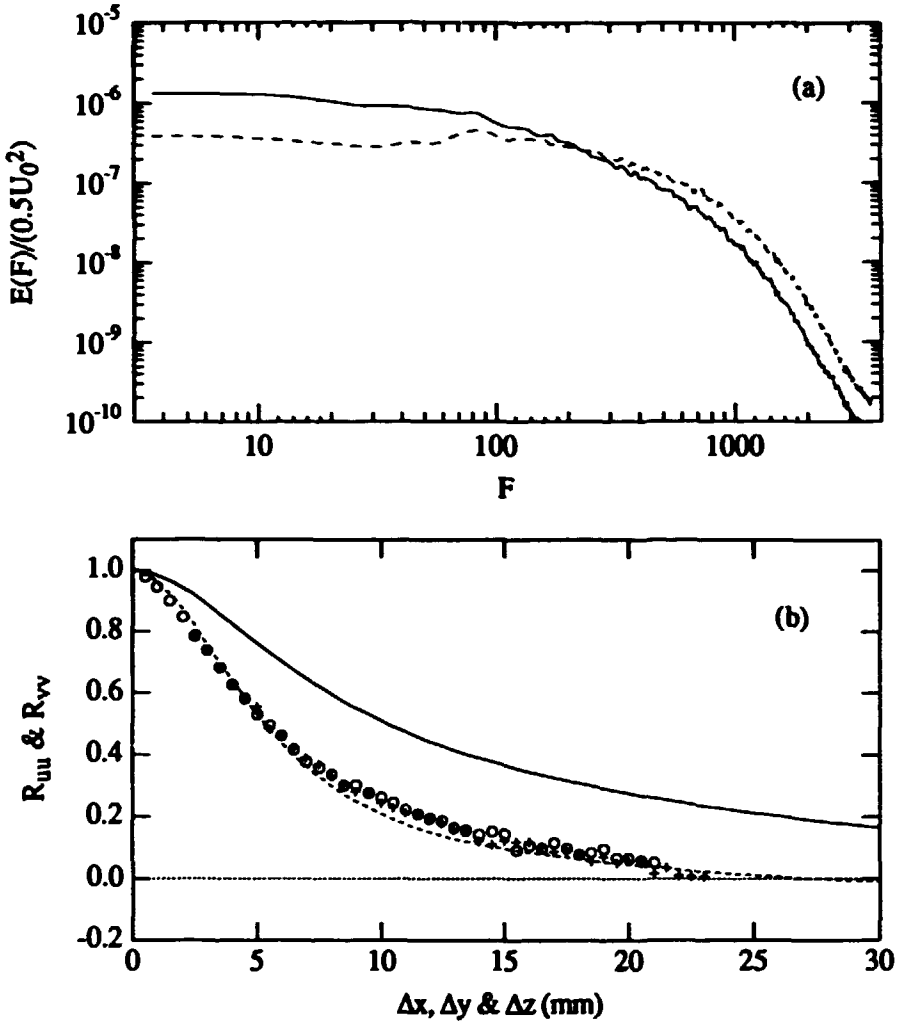


Figure 4: (a) Free stream spectra at $x = 0$, $U_0 = 8$ m/s. (—) $u$- and (- - -) $v$-component. (b) Free stream correlations at $x = 500$ mm, $U_0 = 8$ m/s. Autocorrelation of (—) $u$- and (- - -) $v$-component. Cross correlations with (o) $\Delta y$ and (+) $\Delta z$ probe separations.

$$\tau_u = \sqrt{2}\frac{u_{rms}}{(\frac{\partial u}{\partial t})_{rms}}$$

and similarly for the $v$-component. This expression can be derived from a Taylor series expansion of the correlation function (c.f. Hinze, 1975). $\partial u/\partial t$ was approximated by $\Delta u/\Delta t$ and successively decreasing $\Delta t$ (increasing the sampling frequency) until a limit was reached where cancellation effects became visible. $\tau_u^2$ was then obtained from extrapolation to the limit $\Delta t \rightarrow 0$, by fitting a second degree polynomial to $\tau_u^2$ as a function of $\Delta t$. At $x = 0$, the longitudinal and transverse micro scales were calculated to $\tau_u = 0.87$ ms and $\tau_v = 0.57$ ms ($U_0 = 8$ m/s), which gives a ratio of 1.53. The theoretical ratio for isotropic turbulence is $\sqrt{2} = 1.41$. The corresponding transverse length scale ($\lambda_v$) is 4.6 mm. As a consequence of the dissipation of the smallest scales, the length scales increase downstream. At $x = 500$ and 1000 mm, the values of $\lambda_v$ are 5.2 and 5.9 mm respectively.

The integral length scales ($\Lambda_u$ and $\Lambda_v$), are usually calculated by integrating the autocorrelation functions shown in figure 4b over all separations. However, the integrated values are often ambiguous, because the autocorrelation curve is easily affected by long time fluctuations in the mean

velocity, resulting in different integral length scales depending on the chosen sampling parameters. This problem is most evident in the $u$-correlation. Another possibility is to extrapolate the energy density spectra $E(F)$ to $F = 0$. The integral time scale is then obtained as $E(0)$ normalized with $u^2_{rms}$, but also with this method there is a significant arbitrariness when the extrapolation is carried out. By extrapolating the $v$-spectra, $\Lambda_v$ was estimated to be within 7-10 mm along the flat plate, and the corresponding $\Lambda_u$ was 2 to 3 times larger. The rather small ratio between integral and micro scales ($\Lambda_v/\lambda_v$) may be explained by the small turbulent Reynolds number ($Re_\lambda = u_{rms}\lambda_v/\nu \approx 40$).

The downstream development of the free stream fluctuations ($u_{rms,0}$ and $v_{rms,0}$) are shown in figure 5. The typical power-law decay can be described in the form

$$u_{rms,0}/U_0 = C(x - x_0)^b,$$

where $x_0$ is a virtual origin. A curve fit of this form to the data measured at $x \geq 0$ gave an exponent $b = -0.62$, in fair agreement with other investigations of grid generated turbulence, e.g. Baines & Petersen (1951) obtained $b = -0.71(-5/7)$ and Groth & Johansson (1988) $b = -0.5$. If it is assumed that the decaying turbulence can be described by the k-$\epsilon$ model, the exponent can easily be derived if the turbulent diffusion terms are neglected. This would give an exponent of -0.54 for the empirical coefficient $c'_{\epsilon 2} = 1.92(b = 0.5/(1 - c'_{\epsilon 2}))$. A smaller exponent is obtained if data measured upstream of the leading edge are included, since these are more affected by the anisotropic region near the grid. The ratio between $v_{rms,0}$ and $u_{rms,0}$ has an approximately constant value of 0.9 along the measured region, indicating a minor degree of anisotropy. For comparison, in the experiments of Roach & Brierley (1992), this ratio was reported to be equal to one to within 0.5%.

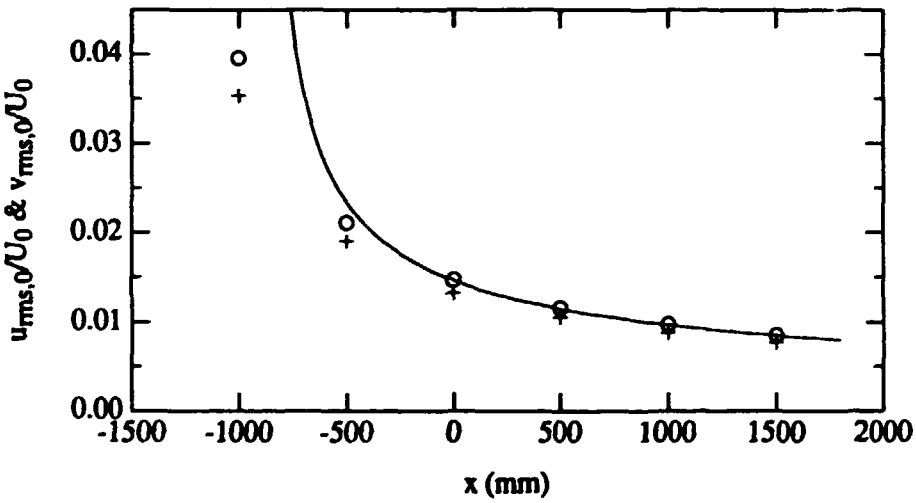


Figure 5: Downstream decay of FST for $U_0 = 8$ m/s. (o) $u_{rms,0}/U_0$, (+) $v_{rms,0}/U_0$, (—) decay curve according to $u_{rms,0}/U_0 = C(x - x_0)^b$ with $b = -0.54$, $x_0 = -871$ mm.

In summary, despite the good agreement between the correlations in all three transverse directions (figure 4b), careful inspection of the parameters studied above (i.e. the ratios $v_{rms,0}/u_{rms,0}$ and $\tau_u/\tau_v$, as well as the exponent $b$), reveals a minor degree of anisotropy in the present set-up. At 8 m/s, typical transverse scales in the free stream range between 4.6 mm (Taylor's micro scale) and 10 mm (integral or macro scale). At 4 m/s, the value of $Tu$ is almost the same. By comparing the autocorrelations of $u$ at 4 and 8 m/s (see figure 3b), the turbulence scales are estimated to be

approximately equal at both velocities. On the other hand, the boundary layer thickness at a given $R$ is $\sqrt{2}$ times larger at 4 m/s than at 8 m/s. This means that the relative size of the free stream eddies compared with the boundary layer thickness are smaller at 4 m/s, a factor which may be of importance for the receptivity of the boundary layer to free stream disturbances.

# 4 Structure of the boundary layer perturbations

In this section we will describe the effect of FST on the mean and fluctuating velocities upstream of the onset of transition. Results from measurements at different $R$ are presented and compared, allowing some conclusions to be made about the downstream development and scaling of the perturbations induced by FST. The measurements at 4 m/s were made in set-up I, which is identical to that reported by Klingmann et al. (1993), whereas the measurements for 8 m/s were obtained in set-up II. At far downstream positions, turbulent spots occurred occasionally. Since the objective of the present study is to document the laminar boundary layer development, sampling records affected by the passage of turbulent spots were rejected.

## 4.1 Mean velocity characteristics of the boundary layer subjected to free stream turbulence

Mean velocity profiles were measured with an equidistant $y$-step of 0.1 mm. The distance between the surface and the first $y$-position was estimated by linear extrapolation of the near wall part of the profile, after discarding points visibly affected by heat conduction to the wall. The boundary layer characteristics (i.e. the displacement thickness $\delta^*$, the momentum loss thickness $\theta$, and the shape factor $H = \delta^*/\theta$) were then evaluated by numerical integration according to Simpson's formula. The accuracy in the value of $H$ obtained from this procedure was estimated to be within $\pm 0.5\%$, but this error does not include possible inaccuracies in the hot wire calibration. Comparisons between profiles measured with different calibrations indicated that the inaccuracy in the evaluation of $H$ may be slightly larger. However, this error limit is well below the observed differences between the cases with and without grid.

Figures 6a and 6b compare boundary layer profiles measured with and without the grid at $x = 450$ mm. The $y$-coordinate is normalized with the measured value of $\delta^*$, given in Table 1. The undisturbed boundary layer has characteristics close to an ideal Blasius flow, whereas the boundary layer subjected to FST shows small but significant deviations. The difference between the velocities measured with and without the grid ($\Delta U/U_0$) at $x = 450$ mm are shown in figures 6c and 6d, and it amounts to about $\pm 1\%$. At both free stream velocities, the presence of the grid gives profiles with larger mean velocity close to the wall, whereas there is a velocity deficit in the outer part of the boundary layer. The perturbed boundary layer profile is qualitatively similar to the profile shape obtained from a negative pressure gradient with the same shape factor. In figures 6c-d, the measured deviations are compared with the difference between a Falkner-Skan profile and a Blasius profile, showing that the measured deviations are found slightly further out in the boundary layer. This was found to be a general trend at all Reynolds numbers studied, and irrespective of whether the comparison is made at a given $y$-position or at a given $y/\delta^*$.

The downstream development of the mean velocity profile at 8 m/s is shown in figure 7a, together with the corresponding Blasius profiles. Three different $x$-positions are shown: $x = 100$, 500 and 1000 mm. A systematic development towards a fuller profile can clearly be observed, whereas the boundary layer thickness is only slightly affected. The maximum in $\Delta U/U_0$ increases with $R$, and amounts to 3–4% at $x = 1000$ mm. Figure 7b shows profiles of $\Delta U$ normalized with

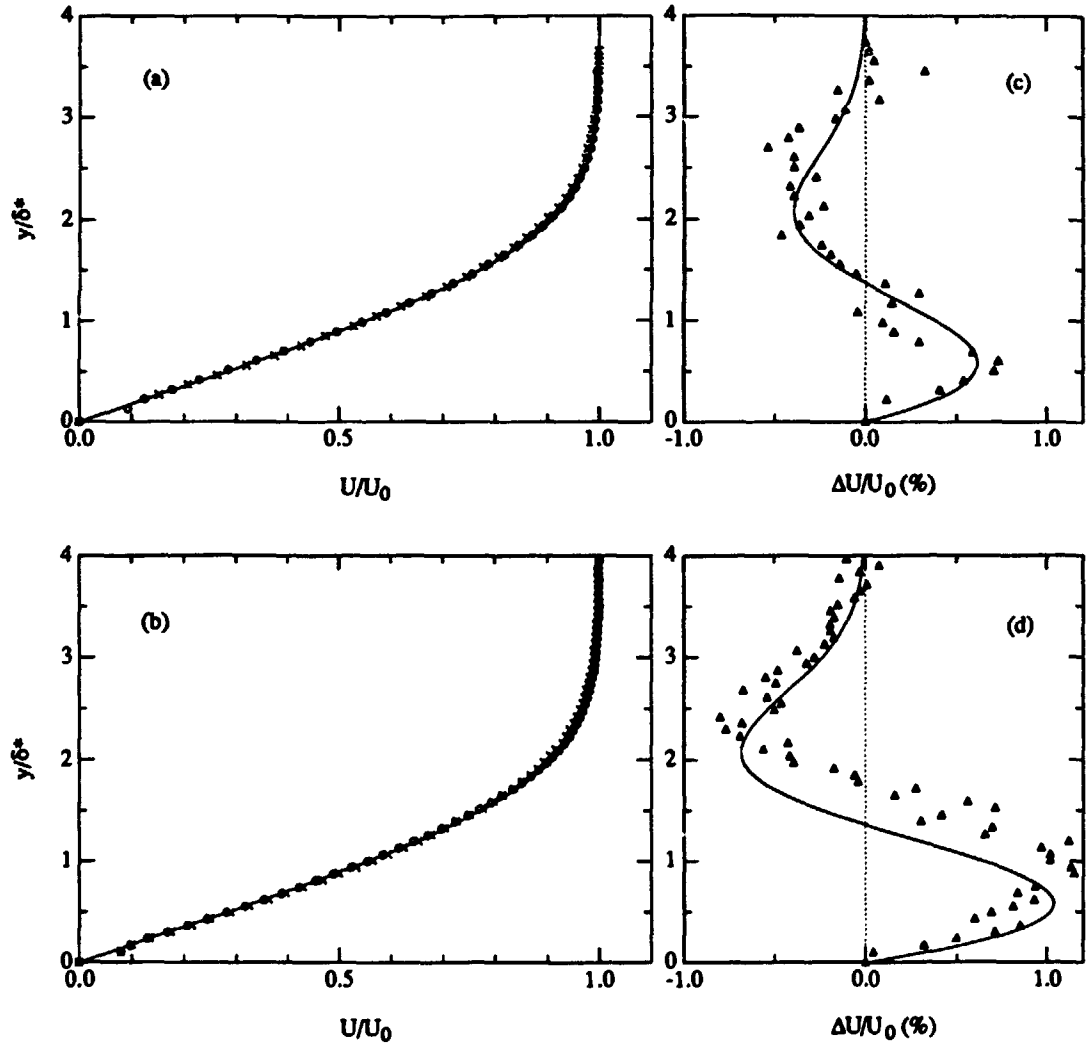


Figure 6: Mean velocity profiles at $x = 450$ mm for (a) $U_0 = 4$ m/s and (b) $U_0 = 8$ m/s: (x), with grid, (o) without grid. Solid lines are Blasius profiles. Velocity changes ($\Delta U$) due to free stream turbulence at $x = 450$ mm for (c) $U_0 = 4$ m/s and (d) $U_0 = 8$ m/s. Solid lines show the difference between Falkner-Skan (with same shape factor as measured profile) and Blasius profiles.

| $x$ (mm) | $U_0$ (m/s) | $\delta^*$ (mm) | $Re_{\delta^*}$ | $1.72\sqrt{Re_x}$ | $H$ |
|---|---|---|---|---|---|
| 450 without grid | 4.1 | 2.27 | 623 | 605 | 2.58 |
| 450 | 4.0 | 2.23 | 587 | 592 | 2.55 |
| 450 without grid | 8.0 | 1.560 | 827 | 840 | 2.58 |
| 450 | 8.1 | 1.553 | 834 | 846 | 2.53 |

Table 1: Boundary layer characteristics.

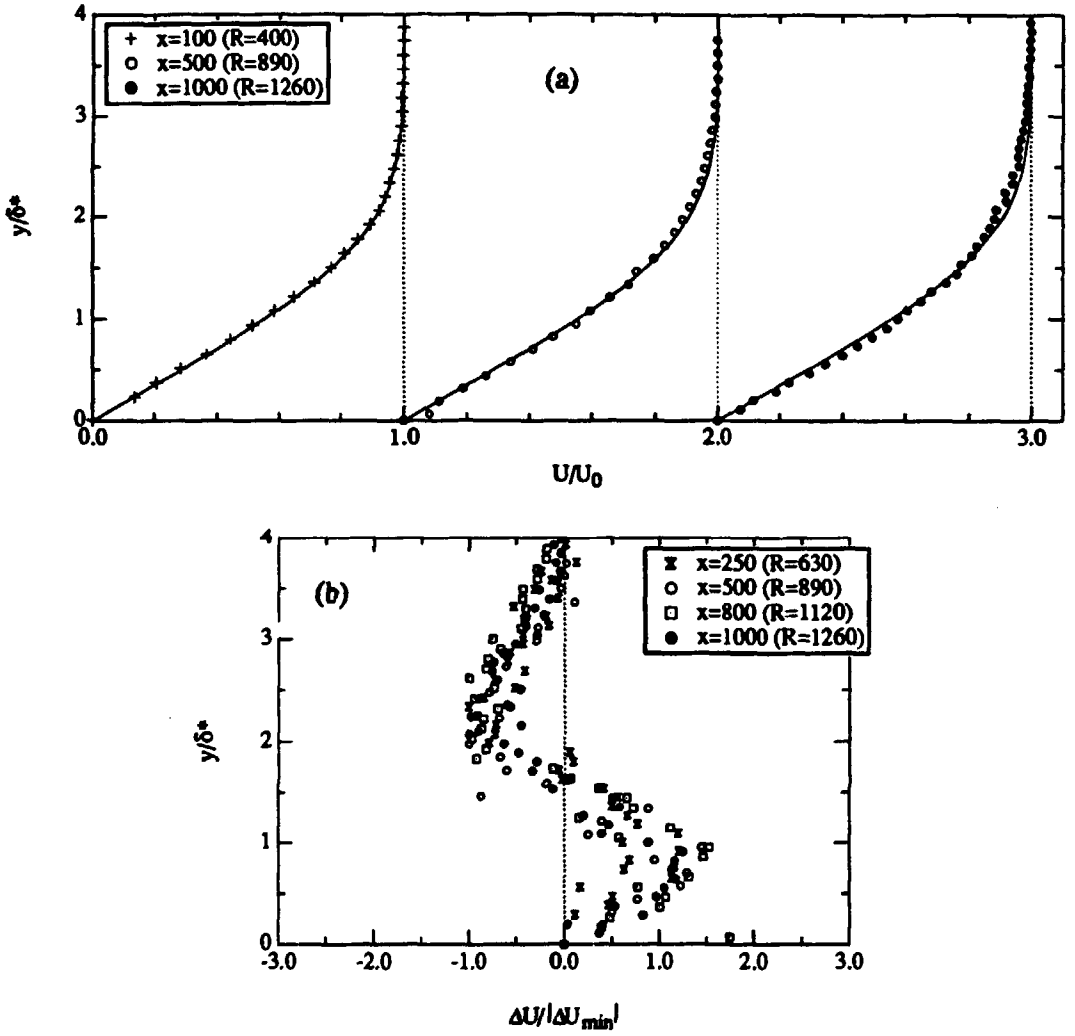


Figure 7: (a) Mean velocity profiles with grid at $U_0 = 8$ m/s. Solid lines are Blasius profiles. (b) Normalized mean velocity deviations compared with Blasius.

| $x$ (mm) | $U_0$ (m/s) | $\delta^*$ (mm) | $Re_{\delta^*}$ | $1.72\sqrt{Re_x}$ | $H$ |
|---|---|---|---|---|---|
| 100 | 8.0 | 0.715 | 381 | 397 | 2.61 |
| 250 | 8.0 | 1.125 | 600 | 628 | 2.54 |
| 500 | 8.0 | 1.573 | 839 | 888 | 2.48 |
| 800 | 8.0 | 2.044 | 1090 | 1124 | 2.43 |
| 1000 | 8.0 | 2.251 | 1200 | 1256 | 2.41 |

Table 2: Boundary layer characteristics.

its minimum value, and the shape is fairly selfsimilar at all measured stations.

The values of $H$ corresponding to figure 7 are given in Table 2, and their variation with $R$ is plotted in figure 8, showing that the shape factor decreases linearly with $R$. The slope is the same both at 4 m/s and 8 m/s, suggesting that the downstream evolution of $H$ may be insensitive to the details in the free stream conditions. The changes in $H$ are mainly due to a downstream decrease in $\theta$ in comparison with the Blasius case, whereas $\delta^*/1.72\sqrt{\nu x/U_0}$ is fairly constant. This observation is also consistent with the measured shape of $\Delta U$ (figure 7b). Integration of $\Delta U$ over the boundary layer thickness gives approximately zero for all profiles, i.e. the FST does not change the mass flow in the boundary layer compared with a Blasius profile. Although the value of $H$ at $R = 1260$ ($x = 1000$ mm) is as small as 2.41, this point can still be considered as upstream of the onset of transition, even though turbulent spots occur occasionally. It should be noted that the deviation from the Blasius flow is not due to turbulent intermittency, but reflects the motion of large scale structures embedded in the boundary layer. The clear difference between these non-turbulent structures and turbulent spots will become evident from the study of the boundary layer fluctuations in the following subsection.

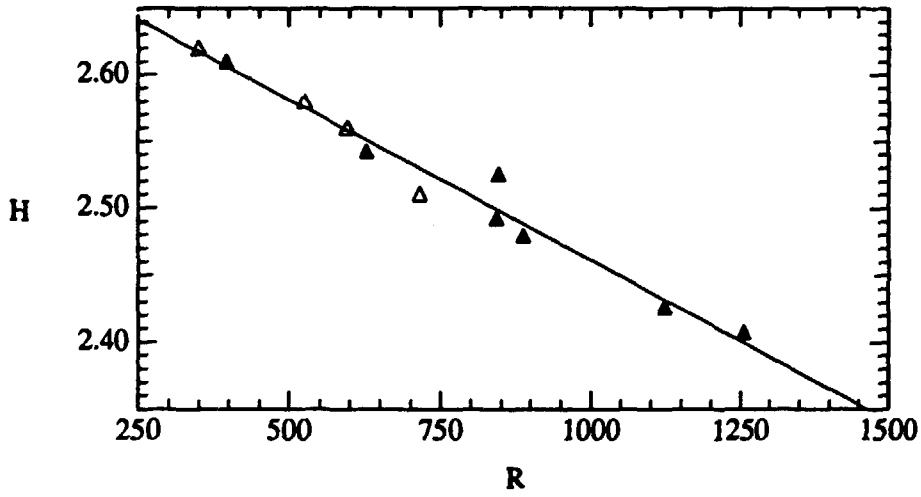


Figure 8: Downstream development of the shape factor $H$. ($\Delta$) $U_0 = 4$ m/s, ($\blacktriangle$) $U_0 = 8$ m/s.

## 4.2 Fluctuating velocity

In order to gain more insight into the nature of the boundary layer perturbations caused by FST, the $u$-fluctuations were analyzed at several downstream positions and for two different free stream velocities. Figure 9a shows profiles of $u_{rms}$ for $U_0 = 4$ m/s. Near the boundary layer edge, the amplitude is approximately equal to that in the free stream, and it decreases slowly from 1.35% at the leading edge to 1.1% at $x = 650$ mm ($R = 715$). In contrast, inside the boundary layer the fluctuations are several times larger, and they increase with downstream distance to a value of about 5% at $R = 715$. The rms-profile scales approximately with $\delta^*$, and its maximum ($u_{rms,max}$) is near $y/\delta^* = 1.4$. At 8 m/s and $Tu = 1.5\%$ (figure 9b), the shape of the rms-profile is similar, but with the maximum slightly closer to the wall, $y/\delta^* = 1.2$. While the rms-values at the boundary layer edge is slowly decreasing, the boundary layer fluctuations increase to 11% at $x = 1000$ mm ($R = 1260$). The variation of $u_{rms,max}/U_0$ with $x$ is shown in figure 10 for both velocities. It can be seen that $u_{rms,max}$ varies linearly with $R$, but the slope is different for the two cases. Also if

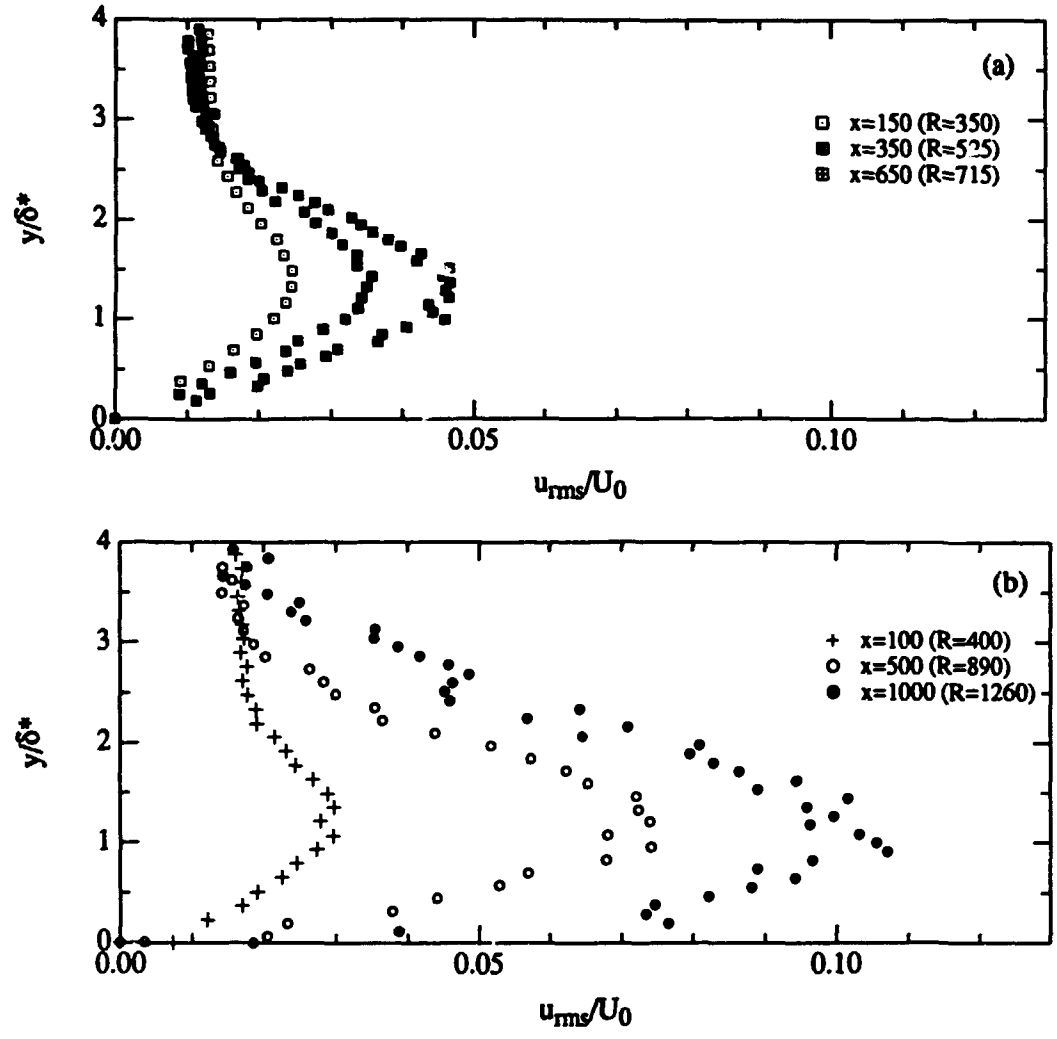


Figure 9: Profiles of total $u_{rms}$ fluctuations at different $R$. (a) $U_0 = 4$ m/s, $Tu = 1.35\%$, (b) $U_0 = 8$ m/s, $Tu = 1.5\%$.

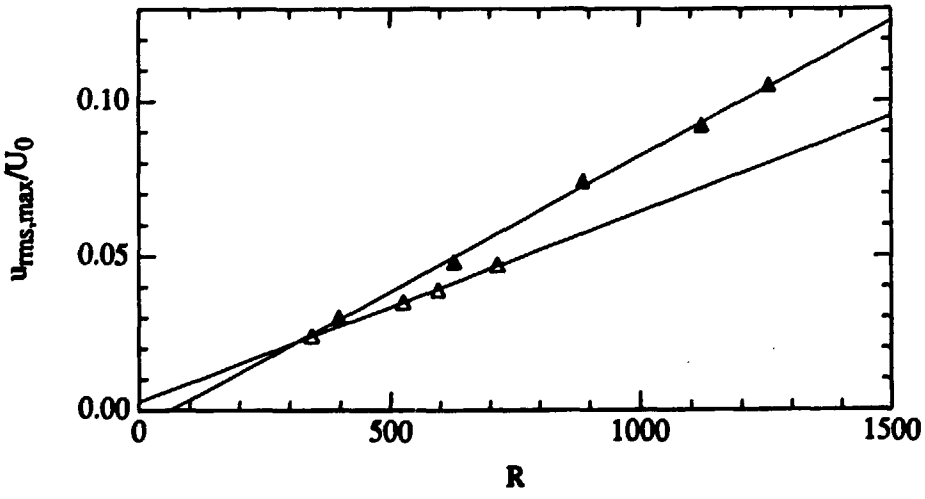


Figure 10: Downstream development of $u_{rms,max}$. ($\Delta$) $U_0 = 4$ m/s, ($\blacktriangle$) $U_0 = 8$ m/s.

$u_{rms,max}$ is scaled with $Tu$ and $U_0$, there is a larger growth rate for the higher free stream velocity. This may indicate a change in the receptivity to FST when the free stream velocity is changed, due to a change in the relative size of free stream and boundary layer scales.

Figure 11 shows frequency spectra at different $y$-positions measured at $x = 500$ mm and $U_0 = 8$ m/s. The spectra correspond to the middle of the boundary layer (where $u_{rms}$ is maximum), the near wall region (where TS-waves would have their maximum), and in the free stream. Whereas the free stream energy is smoothly distributed over frequencies up to several hundred Hz, the energy distribution in the boundary layer is strongly concentrated at low frequencies, and this is seen more clearly when the wall is approached. This may be interpreted as that the boundary layer selectively amplifies low frequency fluctuations from the free stream. Another view, which will be substantiated in the following, is that the perturbations entering the boundary layer at some upstream position are continuously elongated by the mean shear, leading to stretched structures, which are seen as low frequency fluctuations. Higher frequencies may be the result of random motions of such structures. Suppose that the structures move at a velocity equal to the local mean velocity at $u_{rms,max}$, i.e. about $0.7U_0$. A frequency of 100 Hz at 8 m/s would then correspond to a structure with a length of 55 mm, and 10 Hz would correspond to 0.55 m, i.e. the order of $x$. It should also be emphasized that the previously described boundary layer disturbances are not influenced by turbulent spots. If measurements are carried out without spot sorting in the region of transition onset, the boundary layer spectra will show an increase in energy over all frequencies, and the corresponding rms-profile will show a large amplitude maximum near the wall due to the turbulent spots.

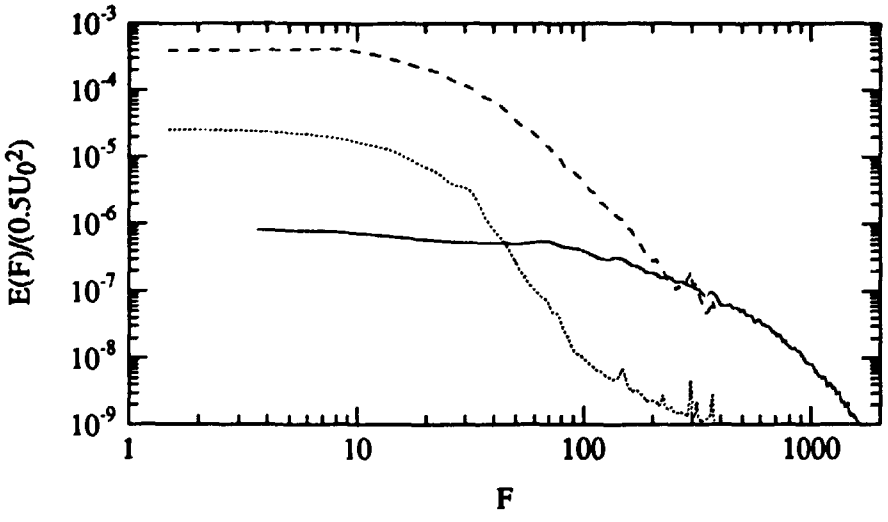


Figure 11: Energy density spectra for $u$ at different wall-normal positions at $x = 500$ mm, $U_0 = 8$ m/s ($R = 890$). (—) free stream, (- - -) middle of the boundary layer, ($\cdots$) near wall region.

Figure 12 shows profiles of the energy contributions to $u_{rms}$ from selected narrow frequency bands. Two $x$-positions are shown, $x = 500$ mm and $x = 1000$ mm for $U_0 = 8$ m/s. With increasing frequency, the energy maximum with respect to $y$ is shifted further out in the boundary layer. This is in agreement with observations made by Kosorygin et al. (1982) under similar conditions. This monotonous trend suggests the existence of a specific type of structure, rather than a combination of modes. The frequency band $F = 75$ represents typical TS-wave frequencies at these Reynolds numbers, and its shape displays no special features in this context. Its maximum is in the outer

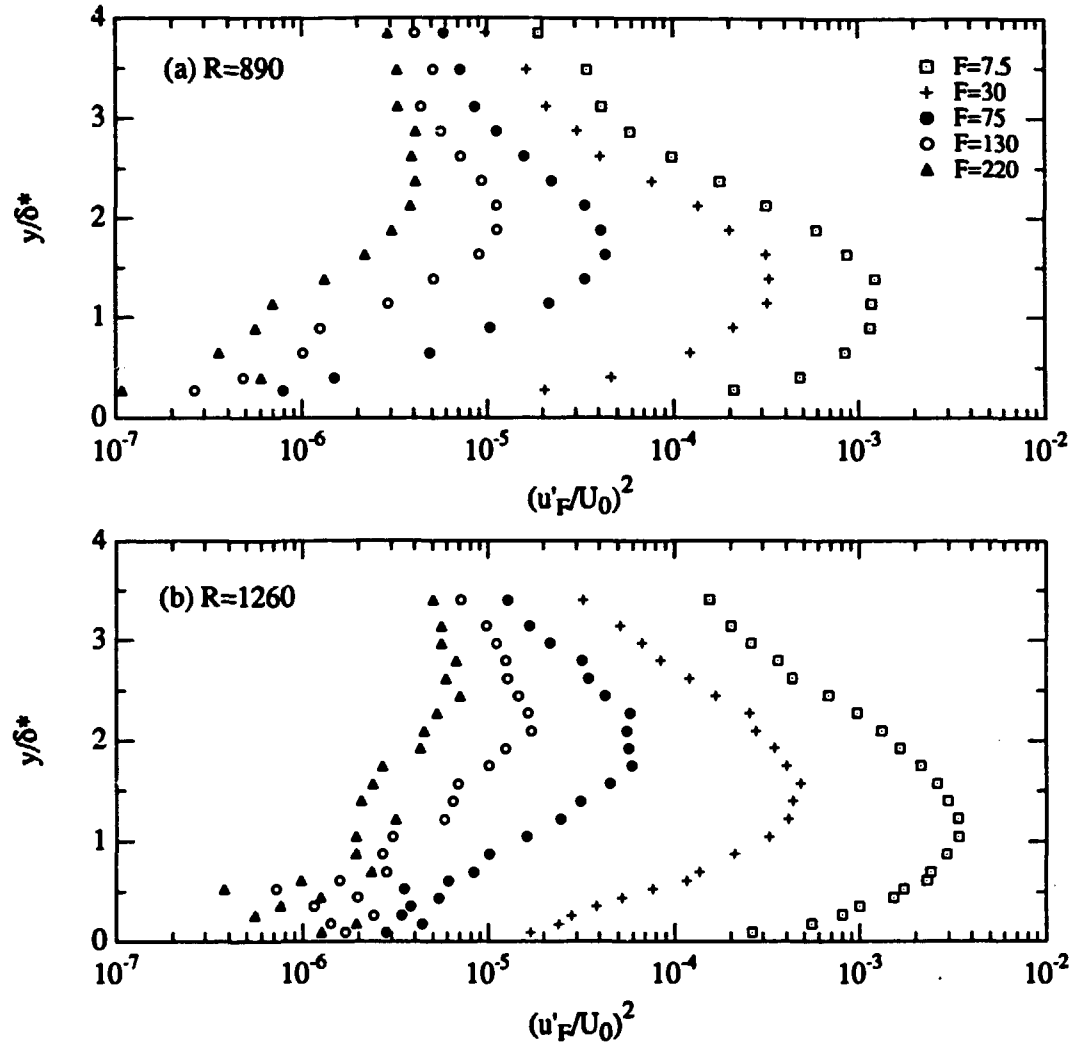


Figure 12: Profiles of fluctuating energy in frequency bands at $U_0 = 8$ m/s. (a) $x = 500$ mm, ($R = 890$), (b) $x = 1000$ mm ($R = 1260$).

part of the boundary layer, and there is no evidence of a near wall maximum typical for TS-waves. However, this observation does not allow any conclusion about the existence or non-existence of TS-waves. At the present level of FST, it would be impossible to detect naturally occurring TS-waves by merely looking at rms-spectra, since these are dominated by other fluctuations with much larger amplitudes. Another interesting observation is the downstream increase of the energy close to the boundary layer edge for higher frequencies. This is most evident in the profiles for $F \geq 75$, where the energy maximum is approximately constant at the two downstream positions, while the energy at $y/\delta^* \approx 3$ shows a significant increase. This is also consistent with oscilloscope observations, where higher intermittency was observed close to the boundary layer edge.

As seen in figure 12, most of the energy is concentrated at $F$ below 30, whereas the energy at higher frequencies gives only small contributions to $u_{rms}$. For $F \geq 220$, the energy inside the boundary layer does not exceed that in the free stream. The downstream growth of $u_{rms}$ is mainly due to an increase of energy at $F$ below 30, whereas it is almost constant for higher frequencies. At the $u_{rms}$-maximum with respect to $y$, the energy in the band $F = 7.5$ is seen to increase by a factor of 3 between the two $x$-positions. (For comparison, the free stream energy in this band

is approximately constant). The $u_{rms}$ plots in figure 12b show that the corresponding increase in the total energy is only a factor of 2, which means that energy is redistributed from high to low frequencies. If the low frequency components are supposed to represent the motion of longitudinal streaks in the boundary layer, it means that the streaks not only grow in amplitude but also elongate as they travel downstream. The redistribution of energy to lower frequencies is seen more clearly in figure 13, which shows the ratio between the upstream and downstream energies ($E_\delta|_{x=1000}/E_\delta|_{x=500}$), where $E_\delta(F)$ is the fluctuating energy at the frequency $F$ ($u_F'^2$) integrated through the boundary layer ($\delta$ was here taken as 10 mm at both positions):

$$E_\delta(F) = \int_0^\delta u_F'^2 dy$$

The energy increase at low frequencies is partly compensated by a decrease at $F$ between 30 and 60, while the energy at higher frequencies is constant.

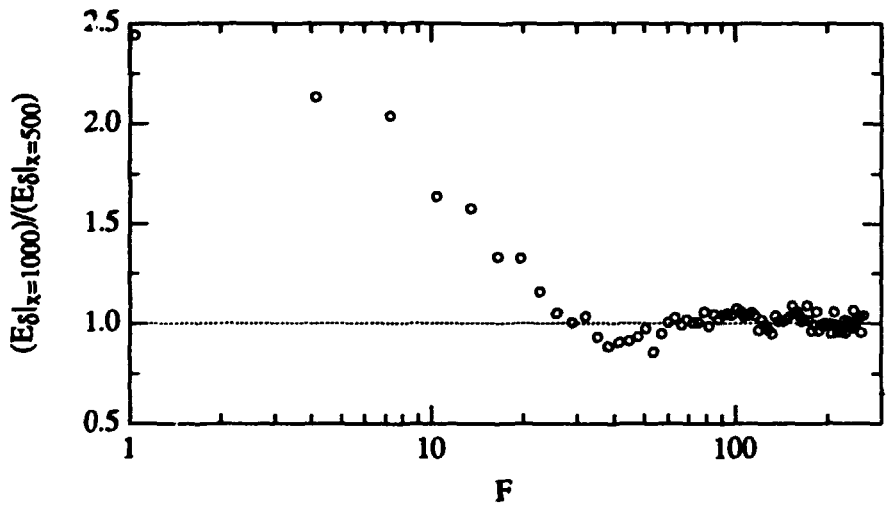


Figure 13: Ratio of the fluctuation energy integrated across the boundary layer at $x = 1000$ ($R = 1260$) and $x = 500$ ($R = 890$). $U_0 = 8$ m/s.

The spanwise distribution of the boundary layer perturbations can be assessed by measuring the correlation between two hot-wires displaced in the spanwise direction. Previous authors (cf. Kendall, 1985; Kosorygin & Polyakov, 1990) have observed a clear anti-correlation at a certain spanwise probe separation, approximately the size of the boundary layer thickness. Visualizations by Kendall, showed spanwise streak formations separated about twice the distance of the measured minimum in the spanwise correlation. This gives a clear indication of the existence of longitudinal streak structures in the boundary layer, and the measured scale corresponds to half of their average spacing. Figure 14 shows correlations obtained in the present set-up at $x = 500$ ($R = 890$) and $x = 1000$ ($R = 1260$), and they were measured at the $y$-position where $u_{rms}$ has a maximum (the corresponding correlation in the free stream is also included for reference). The correlations reaches a value of $-0.3$ at a spanwise separation of about 5.5 mm at $R = 890$ and 6.5 mm at $R = 1260$. This is of the order of the boundary layer thickness (4.8 and 6.8 mm at the respective x-positions), but also matches the transverse scales of the free stream turbulence ($\lambda_v = 5.2$ and 5.9 mm, and $\Lambda_v \approx 7 - 10$ mm at both positions). The ratio between the spanwise scales in the boundary layer

is smaller than the ratio between the boundary layer thickness at the two positions, but slightly larger than the ratio between the micro scales. Hence, from the present measurements it is difficult to draw any conclusions about what determines the spanwise scales.

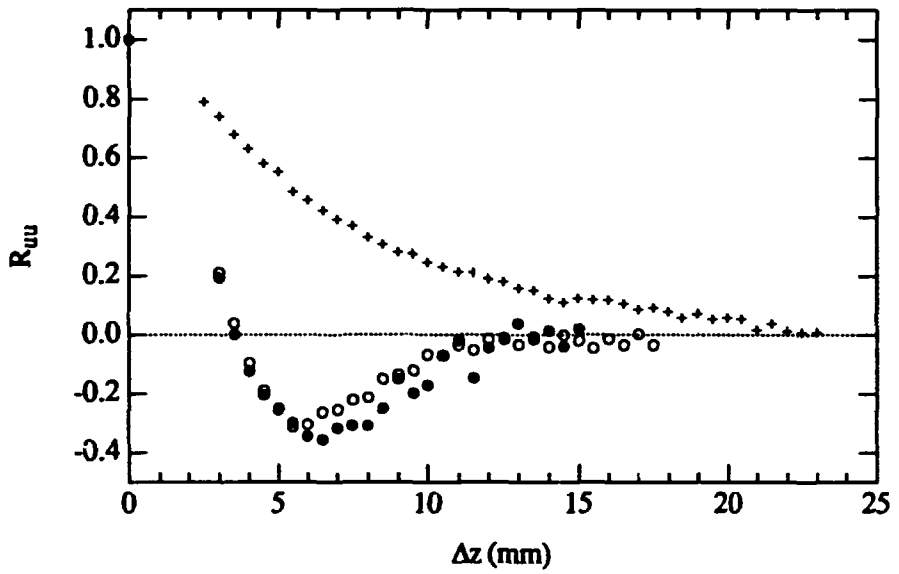


Figure 14: Spanwise correlations in the boundary layer, measured close to the maximum of $u_{rms}$ for $U_0 = 8$ m/s: (o) $x = 500$ mm ($R = 890$), (•) $x = 1000$ mm ($R = 1260$). (+) Spanwise correlation in the free stream ($x = 500$ mm)

# 5 Discussion and comparison with other experiments

The results presented above will be compared with results obtained by other authors at different free stream conditions, so that further conclusions can be drawn about the parameters involved in the receptivity of the boundary layer to FST. The modification of the boundary layer mean velocity in the presence of FST was found to give an increase in the wall shear stress, and a velocity defect in the outer part of the boundary layer. Only few authors have previously reported measurements of $U$ in the laminar region upstream of the onset of transition, and different observations are in disagreement. In the experiment of Kendall (1985), FST was generated with vertical rods placed in the stagnation chamber, giving a turbulence intensity $Tu$ of 0.12% in the test section (the intensity in $v$ was probably larger due to the suppression of $u$ in the contraction). $\Delta U$ was evaluated from measurements made with the grid first present and then absent. Kendall reported a deviation of about 1.5%, measured at $R = 1685$. The $y$-distribution of $\Delta U$ given by Kendall is quite different from that found in the present experiment - it shows a velocity deficit throughout the boundary layer (not only in the outer part), which means that the wall shear stress is smaller than in the undisturbed boundary layer. The results of Roach & Brierley (1992) do not allow a direct comparison of the mean velocity profiles with and without the grid installed. However, the mean profiles obtained in the T3A and T3AM test cases ($Tu = 3\%$ and 1% respectivelty) were compared with a Blasius profile, showing qualitatively the same mean flow deviation as in the present experiment. Also in experiments by Dyban, Epik & Suprun (1976), carried out at different $Tu$ ranging from 0.3% to 12%, a clear increase of the wall shear stress was observed, as well as a

velocity deficit in the outer part of the boundary layer.

In the present experiment, the shape factor was found to decrease linearly with $R$ at a rate independent of the free stream velocity. The same conclusion can be drawn by comparing the shape factors measured by Arnal & Juillen (1978) and Roach & Brierley (1992) which were measured at almost the same level of $Tu$ (0.85% and 1% respectively), but at different $U_0$. Their $H$-values are plotted in figure 15 together with the values obtained here and those of Roach & Brierley for $Tu = 3\%$. The decrease in $H$ within the laminar region is seen to depend mainly on $Tu$, and not strongly on the detailed structure of the FST.

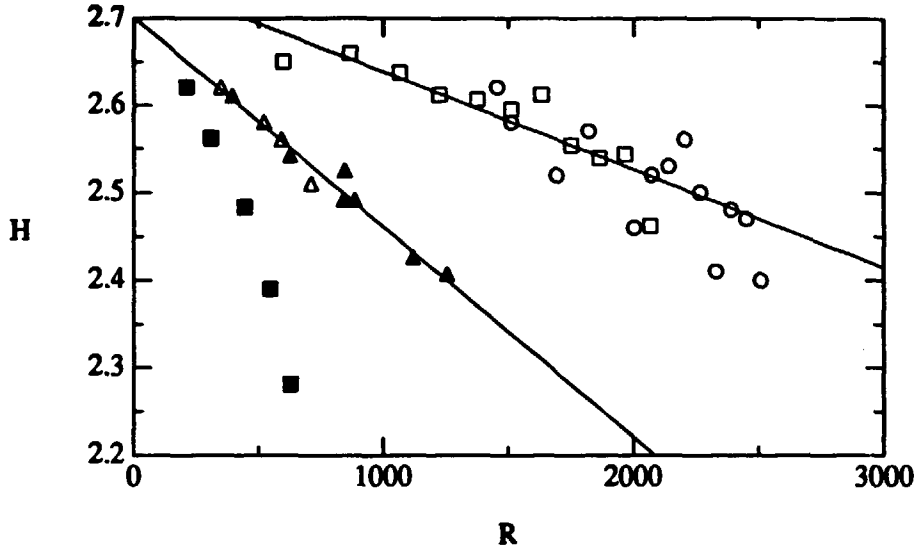


Figure 15: Comparison of the downstream development of the shape factor ($H$) in different experiments. Present results: ($\Delta$), $U_0 = 4$ m/s, $Tu = 1.35\%$, ($\blacktriangle$), $U_0 = 8$ m/s, $Tu = 1.5\%$. T3A (Roach & Brierley): ($\blacksquare$), $Tu = 3\%$, ($\square$), $Tu = 1\%$. Arnal & Juillen: (o), $Tu = 0.85\%$

A comparison of measurements of the fluctuations in the boundary layer with previous authors' results shows qualitative agreement. The dominance of low frequencies inside the boundary layer, as well as the downstream growth of $u_{rms}$ has been observed by most authors, in accordance with the present results. For a large range of $Tu$, the $u_{rms}$ distributions obtained in different studies have approximately the same shape, and the $y$-position of $u_{rms,max}$ is found to be slightly below the middle of the boundary layer. Its exact position, as well as the rate of downstream growth depends on $U_0$ (and thereby probably on the structure of the FST).

Inspection of the data given by Arnal & Juillen (1978), Kosorygin et al. (1982), and the T3A and T3AM test cases shows a linear increase of $u_{rms,max}$ with $R$, as also observed in the present experiments. However, when comparing results obtained with different types of FST, it is clear that there is no simple relation between the level of rms-fluctuations inside and outside the boundary layer. Figure 16 shows the variation of $u_{rms,max}/(Tu \cdot U_0)$ with $R$ for the studies quoted above (i.e. the ratio between the $u$-fluctuations inside and outside the boundary layer). The rate of growth of this quantity, i.e. the slope of the straight lines connecting the data points for each set of measurements, is of the same order of magnitude in all experiments, showing a general trend for the growth rate of $u_{rms}/U_0$ to increase with $Tu$. However, it can be seen that different experiments with similar FST-levels show quite different growth rates. Some of the parameters used in these experiments are listed in Table 3, together with the approximate location of the transition onset

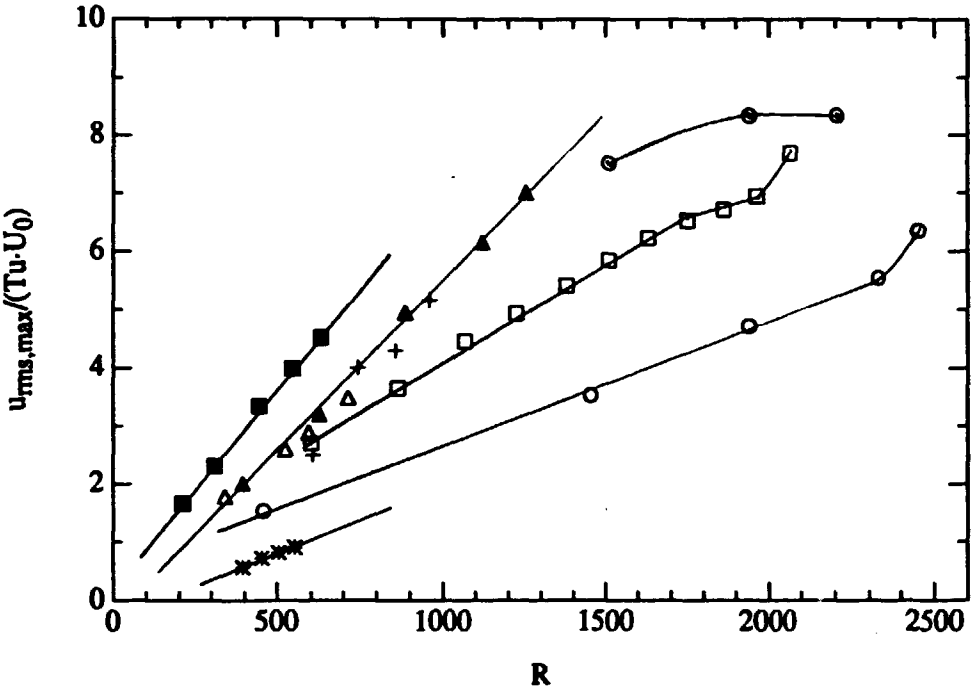


Figure 16: Comparison of the downstream growth of $u_{rms,max}/(Tu \cdot U_0)$ in different experiments. Present results: (Δ), $U_0 = 4$ m/s, $Tu = 1.35\%$, (▲), $U_0 = 8$ m/s, $Tu = 1.5\%$. T3A (Roach & Brierley): (■), $Tu = 3\%$, (□), $Tu = 1\%$. Arnal & Juillen: (o), $Tu = 0.85\%$, (e), $Tu = 0.12\%$. Kosorygin et al.: (+), $Tu = 1.4\%$, (⋆), $Tu = 3.2\%$.

| | $Tu$ (%) | M (mm) | $U_0$ (m/s) | $R_T$ | $\frac{u_{rms,max}}{U_0}$ at $R_T$ (%) |
|---|---|---|---|---|---|
| Arnal & Juillen (1978) | | | | | |
| No grid | 0.12 | | 29 | 2250 | 1.5 |
| Grid 1 | 0.85 | 2.3 | 29 | 2450 | 5.5 |
| Grid 2 | 1.1 | 3.1 | 29 | 1500 | 7 |
| Roach & Brierley (1992) | | | | | |
| T3AM | 1 | 4.2 | 19.8 | 2100 | 7.5 |
| T3A | 3 | 25.4 | 5.4 | 600 | 11 |
| Present results | | | | | |
| 8 m/s | 1.5 | 23.5 | 8.0 | > 1300 | > 11 |
| Suder et al. (1988) | | | | | |
| grid 0.5 | 0.65 | (22.4+screen) | 30.5 | 1200 | 5.5 |
| grid 1 | 0.9 | 22.4 | 30.5 | 1200 | 6.5 |
| grid 2 | 2 | 65 | 30.5 | < 850 | 9 |

Table 3: Comparisons of different experimental studies.

($R_T$) and the corresponding maximum in the $u_{rms}$-level. As observed, both $R_T$ and $u_{rms,max}$ show large differences between the experiments, although the experimental parameters are quite similar in some cases.

The existence of a well defined spanwise scale has also been observed in several studies. This scale can be interpreted as the average spacing between longitudinal structures in the boundary layer, and it would be of interest to clarify if it is determined primarily by the free stream conditions, or by some mechanism inherent to the growth of these structures inside the boundary layer. This is, however, not possible to deduce from the present data, since the spanwise scale inside the boundary layer approximately matches both the typical turbulence scales in the free stream and the boundary layer thickness. Unfortunately, this is also the case in the experiment by Kendall (1985). He presented spanwise correlation functions of $u$ inside and outside the boundary layer at $R = 1740$. The maximum of the spanwise anti-correlation inside the boundary layer was found at $\Delta z \approx 10$ mm, and the boundary layer thickness was about 6.5 mm, which is close to the values obtained here at $R = 1260$. From the spanwise correlation of $u$ in the free stream, the transverse scales can roughly be estimated to 4 and 5 mm (*micro* and *macro* scales respectively), which is smaller than in the present set-up. The ratio between boundary layer scales and free stream scales is then 2-2.5 compared with about 1 in the present case. The fact that similar scales were found inside the boundary layer in both experiments despite the disparity in free stream scales, indicates that there is no direct correspondence between the boundary layer and free stream scales. This is also consistent with an observation of Arnal & Juillen (1978), that the free stream turbulence is poorly correlated with the boundary layer fluctuations.

An important observation to be made from Table 3 is the fact that $u_{rms,max}$ is poorly correlated with the onset of transition. This seems to indicate that the low frequency fluctuations which dominate $u_{rms}$ are not directly responsible for transition. It can also be seen that the value of $Tu$ is not sufficient to predict the onset of transition. This may to some extent be due to effects which are not directly related to the free stream turbulence itself. One such effect might be the leading edge conditions. In the present study, inappropriate leading edge conditions were found to result in a substantial upstream movement of the transition point. The pressure distribution in the presence of the grid is not reported in any of the studies quoted here, but its influence may be appreciated from the value of the shape factor. In most experiments, $H$ is above the Blasius value at upstream positions (see figure 15), which can be the effect of a suction peak near the leading edge. In the experiments by Suder et al., a maximum variation in $C_p$ below 4% was reported, however, the most upstream velocity profiles in their "0.5-grid" case have shape factors above 2.7. Hence, leading edge effects may have been a major reason for the rapid transition observed in their experiments.

# 6 Summary and conclusions

The above observations can be summarized as follows:

(i) The boundary layer perturbations, both in the mean ($\Delta U$) and the fluctuating ($u_{rms}$) velocity field, have a self-similar shape at all $R$. The shape factor decreases linearly with $R$, at a rate which depends on $Tu$, but does not seem to be strongly correlated with the detailed structure of the free stream.

(ii) The $u$-perturbations inside the boundary layer are dominated by large scale, narrow structures, which grow downstream both in length and amplitude. Their streamwise scale is much larger than typical longitudinal scales in the free stream. $u_{rms}/U_0$ grows at a rate proportional to $R$, and in general, the growth rate increases with $Tu$, but depends also on other free stream parameters. There seems to be no direct relation between the value of $u_{rms}/U_0$ in the boundary layer and the

point of transition onset.

(iii) The spanwise scale of the boundary layer perturbations is comparable to the transverse scales in the free stream, however, no direct relation can be established from the available data. Its downstream increase is faster than that of the free stream scales, but slower than that of the boundary layer thickness.

It is not clear to what extent the development of boundary layer fluctuations are due to the dynamics inside the boundary layer, and to what extent they are the result of a continuous forcing from the free stream along the boundary layer edge. In future experiments, it is important to give an extensive description of the free stream characteristics. To be able to find correlations between FST and transition, it is necessary to measure both the $u$- and $v$-components in the FST. It is also important to have an unambiguous estimate of the turbulent scales, to be able to compare different experiments. For instance, it may be possible to conclude something about the spanwise selection mechanism if the FST-scales are compared with the scales in the boundary layer. Experimental set-ups, in which these scales are of clearly different sizes, could be of particular interest.

The observed low frequency structures are similar to the 'puff' observed by Grek et al. (1985) and the 'incipient spot' studied by Klingmann (1992), e.g. their downstream growth is algebraic (as opposed to the exponential growth of e.g. TS-waves), and their spanwise scale varies more slowly than the boundary layer thickness. This indicates that their development may be governed by the linear mechanism suggested by Gustavsson (1991), Klingmann and Henningson et al. (1993). The similarity betweeen the two cases is not unexpected, since free stream eddies entering the boundary layer may be thought of as localized transient disturbances, which develop in the same way as disturbances initially confined to the boundary layer. Transient disturbances are known to devlop into elongating streak structures in the boundary layer, which decay unless the initial amplitude exceeds a threshold level. However, observations by Grek et al. (1991) show that TS-waves generated by a vibrating ribbon can interact non-linearly with these structures, resulting in the formation of turbulent spots.

Although the amplitude of the low frequency perturbations amounts to several percent downstream, the amplitude is poorly correlated with the onset of transition. This indicates that a transition criterion can not be obtained only from information about the longitudinal structures in the boundary layer. The question can only be answered by taking into account different possible routes to transition and an understanding of their relative importance. Experiments with controlled 'model' disturbances, as well as parametric studies using theoretical and numerical models, are therefore necessary. In an accompanying paper (Part II), the effect of Tollmien-Schlichting wave instability in the present flow is investigated, showing that non-linear interaction may occur also for low TS-wave amplitudes.

**Acknowledgements**

This work was supported by the Swedish Board for Technical Development (NUTEK). The visits of Prof. V.V. Kozlov and Dr. A.V. Boiko to Stockholm and the visit of Dr. B.G.B. Klingmann to Novosibirsk were made possible through the scientific exchange program sponsored by the Swedish Royal Academy of Sciences and the Russian Academy of Sciences. The data obtained by Roach & Brierley at Rolls Royce were generously put to our disposal by Dr. J. Coupland.

## REFERENCES


ARNAL, D. 1992 Transition description and prediction. In *Numerical Simulation of Unsteady Flows and Transition to Turbulence* (ed. O. Pironneau, W. Rodi, I.L. Ryhming, A.M. Savill & T.V. Truong), pp. 303-316. Cambridge Univ. Press.

ARNAL, D. & JUILLEN, J.C. 1978 Contribution expérimentale à l'etude de la receptivité d'une couche limite laminaire, à la turbulence de l'écoulement general. *ONERA Rapport Technique* No 1/5018 AYD, June 1978.

BAINES, W.D. & PETERSEN, E.G. 1951 An investigation of flow through screens. *Trans. ASME* **73**, 467-480.

BLAIR, M.F. 1992 Boundary-layer transition in accelerating flows with intense freestream turbulence: Part 1 - Disturbances upstream of transition onset, *J. F. Eng.* **114**, 313-321.

DYBAN, YE.P., EPIK, E.YA & SUPRUN, T.T. 1976 Characteristics of the laminar boundary layer in the presence of elevated free-stream turbulence. *Fluid Mech. - Sov. Res.* **5**(4), 30-36.

GREK, H.R., KOZLOV, V.V. & RAMAZANOV, M.P. 1985 Three types of disturbances from the point source in the boundary layer. In *Laminar-Turbulent Transition 2* (ed. V.V. Kozlov), pp. 267-272. Springer.

GREK, H.R., DEY, J., KOZLOV, V.V., RAMAZANOV, M.P. & TUCHTO, O.N. 1991 Experimental analysis of the process of the formation of turbulence in the boundary layer at higher degree of turbulence of windstream, *Rep. 91-FM-2, Indian Inst. Science, Bangalore, 560012, India.*

GROTH, J. & JOHANSSON, A.V. 1988 Turbulence reduction by screens. *J. Fluid Mech.*, **197**, 139-155

GULYAEV, A.N., KOZLOV, V.E., KUZNETSOV, V.R., MINEEV, B.I. & SEKUNDOV, A.N. 1989 Interaction of a laminar boundary layer with external turbulence. *Izvestiya Akademii Nauk SSSR, Mekhanika Zhidhkosti i Gaza* **5**, 55-65 (in Russian, English transl. 1990 in *Fluid Dyn.* **24**:5, 700-710).

GUSTAVSSON, L.H. 1991 Energy growth of three-dimensional disturbances in plane Poiseuille flow. *J. Fluid Mech.* **224**, 241-260

HENNINGSON, D.S., LUNDBLADH, A & JOHANSSON, A.V. 1993 A mechanism for bypass transition from localized disturbances in wall-bounded shear flows. *J. Fluid Mech.* **250**, 169-207.

HINZE, J.O. 1975 *Turbulence* Second Edition, McGraw-Hill.

JOHANSSON, A.V. 1992 A low speed wind-tunnel with extreme flow quality - design and tests. In *Proc. ICAS congress 1992.* Paper ICAS-92-3.8.1. Publ. by ICAS and AIAA, pp. 1603-1611.

KENDALL, J.M. 1985 Experimental study of disturbances produced in a pre-transitional laminar boundary layer by weak freestream turbulence. *AIAA Paper* 85-1695.

KENDALL, J.M. 1990 Boundary layer receptivity to freestream turbulence. *AIAA Paper* 90-1504.

KENDALL, J.M. 1991 Studies on laminar boundary layer receptivity to freestream turbulence near a leading edge. In *Boundary layer stability and transition to turbulence* (ed. D.C. Reda, H.L. Reed & R. Kobayashi) *ASME FED* **114**, 23-30

KLINGMANN, B.G.B. 1992 On transition due to three-dimensional disturbances in plane Poiseuille flow. *J. Fluid Mech.* **240**, 167-195.

KLINGMANN, B.G.B., BOIKO A.V., WESTIN, K.J.A., KOZLOV, V.V. & ALFREDSSON, P.H. 1993 Experiments on the stability of Tollmien-Schlichting waves, *Eur. J. Mech/B Fluids* **12**, no 4, 493-514.

KOSORYGIN, V.S. & POLYAKOV, N.PH. 1990 Laminar boundary layers in turbulent flows. In *Laminar-Turbulent Transition 3* (ed. D. Arnal & R. Michel), pp. 573-578. Springer.

KOSORYGIN, V.S., POLYAKOV, N.PH., SUPRUN, T.T. & EPIK, E.YA. 1982 Development of disturbances in the laminar boundary layer on a plate at a high level of free stream turbulence. In *Instability of Subsonic and Supersonic Flows*, pp. 85-92. Institute of Theoretical and Applied Mechanics, Siberian Branch of USSR Academy of Sciences, Novosibirsk. (in Russian)

KOZLOV, V.E., KUZNETSOV, V.R., MINEEV, B.I. & SEKUNDOV, A.N. 1990 The influence of free-stream turbulence and surface ribbing on the characteristics of a transitional boundary layer. In *Near-Wall Turbulence* (Proc. of 1988 Zorian Zaric Mem. Conf., ed. S.J. Kline & N.H. Afgan), pp. 172-189. Hemisphere.

PIRONNEAU, O., RODI, W., RYHMING, I.L., SAVILL, A.M. & TRUONG, T.V. 1992 *Numerical Simulation of Unsteady Flows and Transition to Turbulence*. Cambridge Univ. Press.

ROACH, P.E. & BRIERLEY, D.H. 1992 The influence of a turbulent free-stream on zero pressure gradient transitional boundary layer development. Part I: Test cases T3A and T3B. In *Numerical Simulation of Unsteady Flows and Transition to Turbulence* (ed. O. Pironneau, W. Rodi, I.L. Ryhming, A.M. Savill & T.V. Truong), pp. 319-347. Cambridge Univ. Press.

SUDER, K.L., O'BRIEN, J.E. & RESHOTKO, E. 1988 Experimental study of bypass transition in a boundary layer, *NASA TM-100915*.

YANG, Z.Y. & VOKE, P.R. 1991 Numerical simulation of transition under turbulence. University of Surrey, Dept. Mech. Eng. Rep. ME-FD/91.01